HHS Public Access

Author manuscript

Circ Heart Fail. Author manuscript; available in PMC 2016 July 01.

Published in final edited form as:

Circ Heart Fail. 2015 July ; 8(4): 757–765. doi:10.1161/CIRCHEARTFAILURE.115.002210.

Effects of Intracoronary Infusion of Escalating Doses of Cardiac Stem Cells in Rats With Acute Myocardial Infarction

Xian-Liang Tang, MD[1], **Gregg Rokosh, PhD**[1], **Santosh K. Sanganalmath, MD, PhD**[1], **Yukichi Tokita, MD**[1], **Matthew C. L. Keith, MD**[1], **Gregg Shirk, BA**[1], **Heather Stowers, BS**[1], **Gregory N. Hunt, BS**[1], **Wenjian Wu, MSc**[1], **Buddhadeb Dawn, MD**[2], and **Roberto Bolli, MD**[1]

[1]Division of Cardiovascular Medicine and Institute of Molecular Cardiology, University of Louisville, Louisville, KY

[2]Cardiovascular Research Institute, University of Kansas Hospital & Medical Center, Kansas City, KS

Abstract

Background—Although c-kit^{pos} cardiac stem cells (CSCs) preserve left ventricular (LV) function and structure after myocardial infarction (MI), CSC doses have been chosen arbitrarily and the dose-effect relationship is unknown.

Methods and Results—Rats underwent a 90-min coronary occlusion followed by 35 days of reperfusion. Vehicle or CSCs at 5 escalating doses (0.3×10^6, 0.75×10^6, 1.5×10^6, 3.0×10^6, and 6.0×10^6 cells/heart) were given intracoronarily 4 h after reperfusion. The lowest dose (0.3×10^6) had no effect on LV function and morphology, whereas 0.75, 1.5, and 3.0×10^6 significantly improved regional and global LV function (echocardiography and hemodynamic studies). These three doses had similar effects on echocardiographic parameters (infarct wall thickening fraction, LV end-systolic and end-diastolic volumes, LV ejection fraction) and hemodynamic variables (LV end-diastolic pressure, LV dP/dt_{max}, preload adjusted maximal power, end-systolic elastance, preload recruitable stroke work), and produced similar reductions in apoptosis, scar size, infarct wall thinning, and LV expansion index and similar increases in viable myocardium in the risk region (morphometry). Infusion of 6.0×10^6 CSCs markedly increased post-procedural mortality. GFP and BrdU staining indicated that persistence of donor cells and formation of new myocytes were negligible with all doses.

Conclusions—Surprisingly, in this rat model of acute MI, the dose-response relationship for intracoronary CSCs is flat. A minimal dose between 0.3 and 0.75×10^6 is necessary for efficacy; above this threshold, a four-fold increase in cell number does not produce greater improvement in LV function or structure. Further increases in cell dose are harmful.

Correspondence to. Roberto Bolli, MD, Institute of Molecular Cardiology, 550 S Jackson Street, ACB Bldg, 3rd Floor, Louisville, KY 40202, Tel: (502) 852-1837, Fax: (502) 852-6474 rbolli@louisville.edu.

Disclosures

None.

Keywords

cardiac progenitor cells; myocardial ischemia; myocardial regeneration; left ventricular function; myocardial infarction

Over the past decade, several types of stem/progenitor cells have undergone intensive investigation in preclinical models and clinical trials. Among the various cells tested, c-kit^{pos} cardiac stem cells (CSCs), characterized by the expression of the surface receptor tyrosine kinase c-kit, appear particularly promising.[1] Several groups have reported that administration of CSCs improves LV function and structure after myocardial infarction (MI) in a variety of animal models.[2–7] Using autologous or syngeneic c-kit^{pos} CSCs, we have previously shown that transplantation of these cells attenuates LV dysfunction and remodeling in the settings of both acute and chronic MI in rodents[1, 4, 8–11] and pigs.[12] Encouraging results were obtained in SCIPIO (Stem Cell Infusion in Patients with Ischemic Cardiomyopathy; NCT00474461), a phase I, open-label, randomized study designed to investigate the safety and feasibility of autologous CSC infusion in patients with severe heart failure resulting from ischemic cardiomyopathy.[13, 14] The potential therapeutic utility of c-kit^{pos} CSCs is further supported by the fact that these cells can be isolated from small fragments of cardiac tissue and expanded for subsequent autologous administration.[1, 15, 16]

However, despite these encouraging results, many questions pertaining to the therapeutic efficacy of CSCs remain unanswered. One of the most important is the dose of CSCs, which so far has been chosen rather arbitrarily; specifically, what is the dose-response relationship for CSC therapy? In our previous studies, we found that intracoronary administration of 1×10^6 CSCs produced beneficial effects on LV function and structure in rats after acute[9, 11] and chronic MI.[8] However, the optimal cell dosage for this approach, and whether higher doses would result in greater benefit, remain unknown; as mentioned above, the 1×10^6 dose was chosen arbitrarily. In the current study, we used the same model as in our previous investigation[9] (intracoronary administration of CSCs in rats with acute MI) and infused escalating cell doses to delineate the dose-dependency of the effects of CSCs on cardiac repair. Surprisingly, we found that increasing the dose of CSCs above the therapeutic threshold does not result in greater benefit.

Methods

All animal experiments were performed in accordance with the Guide for the Care and Use of Laboratory Animals published by the U.S. National Institutes of Health (Eighth Edition, Revised 2010) and with the guidelines of the Animal Care and Use Committee of the University of Louisville, School of Medicine (Louisville, KY, USA).

Isolation and expansion of c-kit^{pos} CSCs

c-kit^{pos} CSCs were prepared using a modification of the method described by Beltrami et al.[1] Briefly, cardiac cells were isolated from adult male Fischer 344 rats (4–6 months of age), the non-myocyte population was separated from myocytes by gravity sedimentation, counted (number of cells determined), and centrifuged at 600 g for 10 min at RT. Small

intact cells were resuspended and the cells seeded onto two 150 mm dishes in F12K medium with 5% FBS (HyClone), 10 ng/ml bFGF (Peprotech), and 10 ng/ml LIF (Chemicon) (RCSC medium). After six days of expansion, c-kit^{pos} cells were sorted with magnetic beads using a rabbit c-kit antibody (H-300, Santa Cruz). c-kit^{pos} cells were collected with magnetic beads (Dynal) coated with anti-rabbit IgG and maintained in culture with RCSC medium. The recovery of c-kit^{pos} CSCs was determined by flow cytometry staining with an r-phycoerythrin-conjugated rat monoclonal anti-c-kit antibody (Pharmingen). CSCs were labeled with GFP by lentiviral transduction. GFP^{pos} CSCs were selected by blasticidin resistance. c-kit^{pos} CSCs from passages 4–6 were used in all *in vivo* studies of post-MI CSC transplantation. The purity of sorted cells was determined by FACS.

Experimental MI and cell injection

Induction of MI and intracoronary injection of labeled cells in rats were have been previously.[9, 11] Briefly, Female Fischer 344 rats (age 10–12 weeks; weight 174 ± 8 g) were anesthetized with ketamine (37 mg/kg) and xylazine (5 mg/kg) and mechanically ventilated. Anesthesia was maintained with isoflurane (1–3%). All animals underwent a 90-min occlusion of the left anterior descending coronary artery followed by reperfusion (Figure 1), and the chest was closed. Four hours after reperfusion, rats were reanesthetized, the chest reopened, and a thin catheter (Intracath, 22G, Becton Dickinson) was advanced into the aortic root via the left ventricular (LV) apex.[8, 9, 11] Washed CSCs at doses of 0 (vehicle), 0.3, 0.75, 1.5, 3.0, or 6.0 million ($\times 10^6$) were suspended in 1 ml PBS and injected into the aortic root (Figure 1).[8, 9, 11] Rats were followed up for 35 days after cell application and then euthanized for histological studies. For tracking proliferating cells, rats were fed 5-bromo-2'-deoxyuridine (BrdU) in drinking water during the 35-day follow-up (Figure 1).

Transthoracic echocardiography and hemodynamic measurements

Echocardiography was performed under light anesthesia (pentobarbital, 25 mg/kg, i.p.) as described previously[8, 9, 17]using an HDI 5000 echocardiography machine (Philips Medical Systems, Besl, The Netherlands) equipped with 15-7 MHz linear broadband and 12-5 MHz phased array transducers. Serial echocardiograms were obtained at baseline (BSL, 2 days before coronary occlusion) and at 48 h and 35 days after treatment. Short-axis 2D and M mode images were recorded.[8, 9, 17] Systolic and diastolic anatomic parameters were obtained from M-mode tracings at the midpapillary level. LV volume was calculated by Teichholz formula and the ejection fraction (EF) was calculated by M-mode quantification formula. LV area was measured from short-axis 2D images. All measurements were averaged in three consecutive cardiac cycles and analyzed off-line by a single blinded observer using the COMPACS image analysis software. Hemodynamic measurements were performed at the 35-day follow-up, just before euthanasia, using a 2.0 F Millar's Mikro-Tip® ultra-miniature PV loop catheters (SPR-869; Millar Instruments, Houston, TX) as described.[8, 11] In brief, rats were anesthetized with ketamine (37 mg/kg) and xylazine (5 mg/kg), intubated, and mechanically ventilated. Anesthesia was maintained with 1% isoflurane and the core temperature kept at 37.0°C with a heating pad throughout the study. A 2F PV loop catheter catheter (SPR-869, Millar Instruments) was inserted into the right carotid artery and advanced into the LV cavity. The right jugular vein was cannulated for fluid administration. After 20 min of stabilization, the PV signals were recorded continuously with an ARIA PV

conductance system (Millar Instruments) coupled with a Powerlab/4SP A/D converter (AD Instruments), stored, and displayed on a personal computer. PV relations were assessed by transiently compressing the inferior vena cava with a cotton swab. Parallel conductance from surrounding structures was calculated by injecting a small bolus of 30% NaCl through the jugular venous cannula. LV end-diastolic pressure (LVEDP), dP/dt, preload adjusted maximal power (PAMP), end-systolic elastance (Ees), and preload recruitable stroke work (PRSW) were calculated using the PVAN software program (Millar).

Morphometry and histology

After the hemodynamic measurements, a polyethylene catheter filled with phosphate buffer (0.2 M, pH 7.4) and heparin (100 IU/ml) was advanced to the ascending aorta via the right carotid artery. In rapid succession, the heart was arrested in diastole by injecting 1.0 ml of a mixture of cadmium chloride (100 mM)/potassium chloride (3 M) through the jugular venous cannula. The heart was then excised and perfused retrogradely with phosphate buffer for ~3 min to flush out residual blood in the coronary circulation, followed by perfusion with 10% neutral buffered formalin solution for 15 min. Perfusion pressure was maintained between 60 and 80 mmHg while end-diastolic pressure was kept at 8 mmHg. After perfusion-fixation, the atria and right ventricle were dissected from the left ventricle. The LV weight, volume, and the longitudinal intracavitary axis (LV cavity length) were measured to evaluate LV gross morphology.[8, 11] The heart was cut into four transverse slices (~ 2-mm thick), which were processed, embedded in paraffin, sectioned at 4-μm intervals, and stained with Masson's trichrome, picrosirius red, or antibodies against specific cell markers. Images were acquired digitally and analyzed using NIH ImageJ (1.44p). From the Masson's trichrome-stained images, morphometric parameters including risk area, infarct size, and viable myocardium in the risk were measured in each section.[8, 11] To evaluate cardiac fibrosis, LV sections were stained with picrosirius red and collagen content was quantitated in images taken under polarized light.[8, 11]

Immunohistochemistry

Immunofluorescence staining was performed in formalin-fixed, 4-μm-thick histological sections and analyzed by confocal microscopy for GFP, BrdU, α-sarcomeric actin (α-SA), TUNEL positive nuclei, and isolectin. Engraftment and proliferation in LV cross-sections were assessed by staining with antibodies against GFP or BrdU, respectively, which were then counterstained with α-SA. Capillary density was determined in sections stained with FITC-conjugated isolectin. Apoptotic cells were identified by TUNEL staining. Images were acquired and cells staining positive for each of these markers counted and normalized per mm^2.

Statistical analysis

All data are expressed as means ± SEM. Echocardiographic data were performed by two-way repeated-measures ANOVA followed by Student's t-tests with Bonferroni correction for intra- and inter-group comparisons. All parametric data including morphometric, histologic, immunohistochemical, and hemodynamic data were analyzed by one-way ANOVA followed by the Student's t-tests with Bonferroni correction for inter-group

comparisons. Mortality was analyzed by the χ^2 test. All analyses were conducted with SigmaStat3.5. Values of $P<0.05$ were considered significant.

Results

Exclusions and gross measurements

Of the 82 rats enrolled into this study, 32 died during the course of the experiment (Table). One (in the 0.75×10^6 group) of the 32 rats died of ventricular fibrillation during coronary occlusion and the remaining 31 within 48 h after the intracoronary infusion. The mortality rate was similar among the groups (28.6% with vehicle, 30.0% with 0.3×10^6, 26.7% with 0.75×10^6, 30.8% with 1.5×10^6, and 33.3% with 3.0×10^6) except for the 6.0×10^6 group, in which mortality was 80% (12 out of 15), significantly higher ($P<0.05$) than in the other five groups (Table). Thus, a total of 50 rats (10 in the vehicle, 7 in the 0.3×10^6, 11 in the 0.75×10^6, 9 in the 1.5×10^6, 10 in the 3.0×10^6, and 3 in the 6.0×10^6 group) completed the protocol. Because only three rats survived in the 6.0×10^6 group, and because of the obvious toxicity of this CSC dose, these animals were not included in the analysis of cardiac function and structure.

LV weight and LV/body weight ratio were lower in rats treated with CSCs at doses of 0.75×10^6 or higher compared with the vehicle group. Postmortem gross measurements conducted in the diastolically arrested, perfusion-fixed heart revealed a shorter LV longitudinal axis and a smaller chamber volume in rats receiving $0.75–3.0\times10^6$ CSCs compared with rats receiving vehicle (Figure 2).

Myocardial engraftment of transplanted CSCs

Myocardial engraftment of the transplanted CSCs (or their progeny) was determined by counting the number of GFP^{pos} cells on LV sections after immunofluorescence staining for GFP (Figure 3A). As expected, no GFP signal was detected in the 10 hearts in the vehicle-treated group. GFP^{pos} cells in the 0.75, 1.5, and 3.0×10^6 groups were found in 9/11, 8/9, and 9/10 hearts, respectively, in the risk region, and in 5/11, 6/9, and 5/10 hearts, respectively, in the remote region. Quantitative analysis of the hearts with detectable GFP signals revealed that the number of GFP^{pos} cells increased dose-dependently with the escalating doses both in the risk and remote (noninfarcted) regions (Figure 3B). At any given dose, the number of GFP^{pos} cells was greater in the risk region vs. the remote region; however, in both cases, the absolute number of GFP^{pos} cells was extremely low (<50 cells/10,000 nuclei in the risk region and <20 cells/10,000 nuclei in the remote region) (Figure 3B). Thus, intracoronary infusion of CSCs resulted in a dose-dependent increase in myocardial engraftment at 35 days after transplantation of CSCs, but the number of engrafted cells was minuscule, too low to account for functional or structural benefits.

LV morphometric analysis

Morphometric analysis indicated that neither infarct size nor viable myocardium was altered in the 0.3×10^6 group compared with vehicle (Figure 4). Despite similar risk regions among groups, CSCs at doses of 0.75×10^6 and higher significantly reduced infarct size (54.4±2.1% of the risk region in the vehicle group vs. 45.1±2.0% in the 0.75×10^6, 44.2±2.3% in the 1.5

×10^6, and 43.8±3.7% in the 3.0 ×10^6, P <0.05 for all comparisons), increased infarcted wall thickness (1.44±0.07 mm in the vehicle group vs. 2.03±0.12 in the 0.75 ×10^6 [P<0.01], 1.98±0.16 in the 1.5 ×10^6 [P<0.05], and 2.21±0.14 in the 3.0 ×10^6 [P<0.01]), increased the amount of viable tissue within the risk region (45.6±2.1% in the vehicle group vs. 54.9±2.0% in the 0.75 ×10^6. 55.8±2.3% in the 1.5 ×10^6, and 56.2±3.7% in the 3.0 ×10^6, P <0.05 for all comparisons), and limited LV dilation, as indicated by the LV expansion index (0.83±0.04 in the vehicle group vs. 0.56±0.04 in the 0.75 ×10^6, 0.58±0.05 in the 1.5 ×10^6, and 0.54±0.05 in the 3.0 ×10^6, P<0.01 for all comparisons) (Figure 4). Thus, in terms of morphometric variables, the threshold for CSC efficacy lies between the 0.3 and 0.75 ×10^6 doses; above this threshold, there was no indication of a dose-dependent effect of CSCs as the dose increased from 0.75 to 3.0 ×10^6 (Figure 4).

Collagen content in the risk region was reduced by CSC administration at a dose of 0.75 ×10^6 or higher (P<0.05 vs. vehicle for all groups), but not at the dose of 0.3 ×10^6; again, the reduction did not exhibit a dose-dependent pattern (Figure 5). None of the CSC doses had any effect on collagen in the remote region (Supplemental Figure 1).

Echocardiographic and hemodynamic analyses

At baseline (before MI), all parameters of LV function, measured by echocardiography, were similar among groups (Figure 5). At 48 h after MI, the degree of LV dysfunction did not differ among the groups, indicating that the extent of injury sustained during MI was comparable. As expected, in vehicle-treated rats the infarct wall thickness in systole (IWTs), infarct wall thickening fraction (IW ThF), fractional shortening (FS), and ejection fraction (EF) decreased while LV end-systolic diameter (LVESD), LV end-systolic area (LVAs), and LV end-systolic (LVESV) and end-diastolic volume (LVEDV) increased at the 35-day follow-up compared with baseline (Figure 5). In rats that received 0.3 ×10^6 CSCs, none of these parameters was different from the vehicle group, indicating that this dose is not effective. In contrast, in rats that received a dose of 0.75 ×10^6 CSCs or greater, these parameters were improved, so that the IW ThF, FS, EF, and FAC were greater and the LVESD, LVAs, LVESV and LVEDV smaller compared with vehicle-treated rats (Figure 5B). However, in the groups receiving 0.75, 1.5, and 3.0 ×10^6, there was no discernible dose-dependent pattern with respect to any of these echocardiographic variables at the 35-day follow-up (Figure 5B).

Taken together, the echocardiographic data indicate that CSCs improved LV function when the dose exceeded a threshold between 0.3 and 0.75 ×10^6; increasing the cell dose above 0.75 ×10^6 did not produce greater effects.

Consistent with the echocardiographic data, hemodynamic studies (performed before euthanasia using the conductance [Millar] catheter) showed that the lowest dose of CSCs (0.3 ×10^6) did not alter hemodynamic variables compared with the vehicle-treated group (Figure 6). However, CSCs at doses of 0.75 ×10^6 and greater produced significant improvements in LVEDP, dP/dt_{max}, dP/dt_{max}/EDV, preload adjusted maximal power (PAMP), end-systolic elastance (Ees), and preload recruitable stroke work (PRSW) (Figure 6). As was the case for the echocardiographic data, there was no appreciable difference between doses of 0.75, 1.5 and 3.0 ×10^6.

Cellular apoptosis

The number of TUNEL positive cells was counted in approximately 0.5% of total nuclei in both the risk and remote regions (Figure 7). The 0.75 $\times 10^6$ dose produced a dramatic reduction in apoptotic cells in both regions compared with vehicle; the effects of the 1.5 $\times 10^6$ and 3.0 $\times 10^6$ doses were similar (Figure 7).

Cellular proliferation

BrdU incorporation was analyzed in the vehicle, 0.75 $\times 10^6$, 1.5 $\times 10^6$, and 3.0 $\times 10^6$ groups, in which rats received BrdU in the drinking water during the 35-day follow-up. The total number of BrdU positive ($BrdU^{pos}$) cells was higher in the 3.0 $\times 10^6$ group than in vehicle-treated hearts, both in the risk region and in the remote region (Figure 8B, upper panel). Although the total number of $BrdU^{pos}$ cells was higher in the 0.75 and 1.5 $\times 10^6$ groups than in the vehicle group, the differences were not statistically significant.

Co-staining of tissue with BrdU and α-sarcomeric actin (α-sarc) antibodies showed no $BrdU^{pos}/\alpha\text{-sarc}^{pos}$ cells in the vehicle-treated hearts (Figure 8B, middle panel). A dose-dependent increase was noted in the three CSC-treated groups, both in the risk and remote regions (Figure 8B middle panel). There were no significant differences among groups in the either the risk or the remote region. Further analyses after co-staining with GFP revealed that a minority of the $BrdU^{pos}/\alpha\text{-sarc}^{pos}$ cells expressed GFP, indicating that they were the transplanted cells or their progeny (Figure 8B, lower panel).

Taken together, the BrdU data indicate that administration of escalating doses of CSCs was associated with a dose-dependent increase in the numbers of $BrdU^{pos}$ and $BrdU^{pos}/\alpha\text{-sarc}^{pos}$ cells, suggesting that CSC treatment dose-dependently promoted myocyte proliferation. A minority of newly-formed myocytes were derived from the transplanted CSCs. However, since the absolute numbers of $BrdU^{pos}/\alpha\text{-sarc}^{pos}$ cells were extremely low (<10/10,000 nuclei), it is unlikely that this increase in myocyte proliferation contributed importantly to the beneficial effects of CSCs.

Capillary density

Isolectin-stained capillaries averaged approximately 800/mm^2 both in the risk and remote regions of the vehicle-treated hearts (Supplemental Figure 2). Three escalating doses of CSCs (0.75, 1.5, and 3.0 $\times 10^6$) dose-dependently increased capillary density in both the risk and remote regions; compared with vehicle-treated hearts, the density was significantly higher in the 1.5 $\times 10^6$ and 3.0 $\times 10^6$ groups in the risk region, and in the 3.0 $\times 10^6$ group in the remote region (Supplemental Figure 2).

Discussion

The present study was undertaken to determine whether the effects of CSC therapy follow a dose-dependent pattern. The salient results can be summarized as follows. In rats undergoing intracoronary infusion of syngeneic CSCs after acute MI, i) 0.3 $\times 10^6$ CSCs did not produce any beneficial effect on LV structure or function 35 days later; ii) escalating doses of CSCs (0.75 $\times 10^6$. 1.5 $\times 10^6$, and 3.0 $\times 10^6$) resulted in a dose-dependent increase in

the myocardial engraftment of the transplanted cells at 35 days, but the absolute number of these cells was so low (<50 cells/10,000 nuclei) that it was unlikely to contribute significantly to the beneficial effects of CSC therapy; iii) 6.0 $\times 10^6$ CSCs resulted in significantly higher mortality, possibly due to extensive microembolization; iv) doses of 0.75, 1.5. and 3.0 $\times 10^6$ resulted in improved LV structure, as manifested by a shortened LV longitudinal axis, decreased chamber volume, reduced scar size, thicker infarcted LV wall, restrained LV dilation, reduced fibrosis, and increased content of viable myocardium in the risk region; v) this improvement in LV structure was associated with improved regional and global LV function, as demonstrated by two independent techniques: echocardiography (increased IW ThF, reduced LVESV, and increased LVEF) and hemodynamic studies (lowered LVEDP enhanced dP/dt_{max}, and increased PAMP, Ees, and dP/dt_{max}/EDV); vi) neither the improvement in structure nor the improvement in function associated with 0.75 $\times 10^6$, 1.5 $\times 10^6$, and 3.0 $\times 10^6$ CSCs showed a dose-dependent pattern; vii) all three doses of CSCs reduced apoptosis to a similar extent in both the infarcted and the noninfarcted myocardium; and viii) these three doses produced a dose-dependent increase in the formation of new myocytes and capillaries, but the number of new myocytes was exceedingly low. Taken together, these results lead to the conclusion that, in the rat, the benefits of intracoronary infusion of CSCs after acute MI are not dose-dependent. Although many previous studies have examined the effects of CSCs in rodents,[1, 2, 8, 9, 11, 18–23] to our knowledge this is the first analysis of the dose-dependence of these effects.

The reason for using the rat MI model and this range of CSC doses was that our previous studies demonstrated that intracoronary administration of 1 $\times 10^6$ CSCs produced beneficial effects on LV function and morphology in this same rat model.[8, 9, 11] We used intracoronary infusion of CSCs, rather than intramyocardial injection, for several reasons. Clinically, the technique for intracoronary delivery is similar to that used for coronary angioplasty and allows rapid translation because many interventional cardiologists are well versed with this method.[24] In addition, it is the most popular mode of cell delivery in the clinical setting, especially after acute MI, because it can be done simultaneously during a percutaneous coronary intervention for treating stenotic coronary arteries.[25] It also enables stem cells to be selectively infused into the target area. Finally, intracoronary administration allows the cells to home to and engraft within the areas bordering the infarct zone in a broader, more homogeneous manner.

We found that the lowest dose of CSCs (0.3 $\times 10^6$) was ineffective whereas the three higher doses of 0.75, 1.5, and 3.0 $\times 10^6$ exerted clear beneficial effects on LV function (Figures 5 and 6) and structure (Figures 2, 4, and 5) which, however, were not related to the dose. Thus, the threshold for efficacy in this model is between 0.3 and 0.75 $\times 10^6$; above this threshold, the benefits do not increase as the dose of CSCs increases four-fold (from 0.75 to 3.0 $\times 10^6$). Our echocardiographic results were corroborated by the hemodynamic studies, which provide an assessment of function that is completely independent of echocardiography and that, unlike the echocardiographic data, is based on load-independent variables, i.e., dP/dt_{max}/EDV, PAMP, Ees, and PRSW.

In contrast to the functional data, myocyte and CSC proliferation and capillary density exhibited a dose-related pattern with doses of 0.75, 1.5, and 3.0 $\times 10^6$ (Figure 8 and

Supplemental Figure 2). However, the increase in dose did not produce a proportionate increase in myocyte and CSC proliferation. Furthermore, the absolute cell numbers were extremely small and unlikely to have functional significance: for example, the number of $BrdU^{pos}/\alpha\text{-}sarc^{pos}$ cells was <10/10,000 nuclei, and the number of $BrdU^{pos}/\alpha\text{-}sarc^{pos}/GFP^{pos}$ cells was <4/10,000 nuclei (Figure 8 and Supplemental Figure 2).

The effects of the highest dose of CSCs (6.0×10^6) were not analyzed for two main reasons: first, the group size was too small (n=3) for meaningful statistical analysis, and second, the mortality in the this group was much higher than in the other four groups (80% vs. 27–33%, $P<0.05$ for all groups), making it possible that only the "healthiest" animals (those with either less cardiac injury or better overall conditions) may have survived the CSC infusion, thereby skewing the outcome in a manner that is unrelated to CSCs. Clearly, the maximal dose of CSCs that should be considered for experimental studies is the highest dose that does not cause safety concerns.

Most previous investigators studying the effects of different doses of cells with a regenerative capacity have found a positive dose-efficacy relationship. For instance, intramyocardial injection of escalating doses of human bone marrow-derived $CD34^{pos}$ cells in rats,[26] human undifferentiated mesenchymal stem cells (MSCs) and differentiated cardiomyocyte-like cells (CLCs) in rats,[27] and human cardiospheres in mice[28] has been reported to impart dose-dependent functional and histological benefits. Intravenous delivery of MSCs in a porcine model of MI has also been reported to produce a dose-dependent beneficial effect on cardiac function.[29] The reason for the apparent discrepancy between our study and these previous studies[26–29]is unclear, but may relate to the cell type (CSCs vs. bone marrow $CD34^{pos}$ cells, cardiospheres, MSCs, and CLCs), animal model (rats with reperfused MI vs. mice and pigs with permanent LAD ligation), and other methodological differences. A recent study by Dawkins et al[30] in a porcine model of chronic MI found that intracoronary infusion of cardiosphere-derived cells (CDCs) at escalating doses of 6.25, 12.5, and 25.0×10^6 led to equally enhanced preservation of LV function and tissue remodeling without manifestation of a dose-efficacy relationship. That study resembles ours in the sense that in both cases, no dose dependency was found over a four-fold range of cell numbers ($0.75–3.0 \times 10^6$ in our study, $6.25–25 \times 10^6$ in that study).

One can only speculate as to why a four-fold increase in cell delivery (from 0.75 to 3.0 $\times 10^6$) did not result in greater efficacy. We found that, regardless of the dose, the engraftment of CSCs was extremely low, implying that differentiation of transplanted cells into myocytes did not contribute importantly to the functional and structural effects of CSC therapy. We have previously found that CSCs act mainly via paracrine mechanisms,[8, 11]and it is unclear whether such mechanisms are dose-dependent. If the signals released by CSCs (cytokines, miRs, etc.) are amplified non-linearly by endogenous processes (i.e., if they act as triggers of endogenous repair mechanisms, such as mobilization of resident cardiac stem/progenitor cells), then it is conceivable that increased doses of CSCs may not produce a greater response because the mobilization of repair mechanisms may be unrelated to the magnitude of the stimulus.

In conclusion, this study demonstrates that intracoronary administration of syngeneic CSCs in rats with acute MI results in an improvement in LV function and structure, but the magnitude of this improvement is not dose-dependent. The threshold for efficacy is between 0.3 and 0.75 $\times 10^6$; above this threshold, the beneficial effects of CSCs on LV function and remodeling do not increase over a four-fold range (from 0.75 to 3.0 $\times 10^6$). Higher doses have obvious toxic effects, as demonstrated by the increased mortality associated with the 6.0 $\times 10^6$ dose. Therefore, for practical purposes, the dose-efficacy relationship for intracoronarily administered CSCs in this model is flat. We also found that the engraftment of CSCs is negligible regardless of the dose used; even with the highest safe dose (3.0 $\times 10^6$), engraftment was insufficient to account for the benefits afforded by CSC infusion. These results have obvious implications for the design of studies in rats. If these findings can be extrapolated to humans, they would suggest that increasing the dose of CSCs above a level found to be effective and safe may not lead to increased benefit and could potentially be harmful. Given that increasing the number of cells has inherent limitations in potentiating the beneficial effects of CSC therapy, the focus of our future endeavors should be on increasing the quality and potency of the limited number of cells that can be transferred as well as defining the best individual or combinatorial cell populations to maximize the beneficial outcome of cell-based interventional strategies.

Supplementary Material

Refer to Web version on PubMed Central for supplementary material.

Acknowledgments

Sources of Funding

This study was funded by NIH grant P01-HL78825, 1 UM1 HL-113530, and R01-HL74351.

References

1. Beltrami AP, Barlucchi L, Torella D, Baker M, Limana F, Chimenti S, Kasahara H, Rota M, Musso E, Urbanek K, Leri A, Kajstura J, Nadal-Ginard B, Anversa P. Adult cardiac stem cells are multipotent and support myocardial regeneration. Cell. 2003; 114:763–776. [PubMed: 14505575]
2. Fischer KM, Cottage CT, Wu W, Din S, Gude NA, Avitabile D, Quijada P, Collins BL, Fransioli J, Sussman MA. Enhancement of myocardial regeneration through genetic engineering of cardiac progenitor cells expressing pim-1 kinase. Circulation. 2009; 120:2077–2087. [PubMed: 19901187]
3. Oskouei BN, Lamirault G, Joseph C, Treuer AV, Landa S, Da Silva J, Hatzistergos K, Dauer M, Balkan W, McNiece I, Hare JM. Increased potency of cardiac stem cells compared with bone marrow mesenchymal stem cells in cardiac repair. Stem Cells Transl Med. 2012; 1:116–124. [PubMed: 23197758]
4. Bearzi C, Rota M, Hosoda T, Tillmanns J, Nascimbene A, De Angelis A, Yasuzawa-Amano S, Trofimova I, Siggins RW, Lecapitaine N, Cascapera S, Beltrami AP, D'Alessandro DA, Zias E, Quaini F, Urbanek K, Michler RE, Bolli R, Kajstura J, Leri A, Anversa P. Human cardiac stem cells. Proc Natl Acad Sci U S A. 2007; 104:14068–14073. [PubMed: 17709737]
5. Duran JM, Makarewich CA, Sharp TE, Starosta T, Zhu F, Hoffman NE, Chiba Y, Madesh M, Berretta RM, Kubo H, Houser SR. Bone-derived stem cells repair the heart after myocardial infarction through transdifferentiation and paracrine signaling mechanisms. Circ Res. 2013; 113:539–552. [PubMed: 23801066]
6. Williams AR, Hatzistergos KE, Addicott B, McCall F, Carvalho D, Suncion V, Morales AR, Da Silva J, Sussman MA, Heldman AW, Hare JM. Enhanced effect of combining human cardiac stem

cells and bone marrow mesenchymal stem cells to reduce infarct size and to restore cardiac function after myocardial infarction. Circulation. 2013; 127:213–223. [PubMed: 23224061]

7. Sanganalmath SK, Bolli R. Cell therapy for heart failure: A comprehensive overview of experimental and clinical studies, current challenges, and future directions. Circ Res. 2013; 113:810–834. [PubMed: 23989721]
8. Tang XL, Rokosh G, Sanganalmath SK, Yuan F, Sato H, Mu J, Dai S, Li C, Chen N, Peng Y, Dawn B, Hunt G, Leri A, Kajstura J, Tiwari S, Shirk G, Anversa P, Bolli R. Intracoronary administration of cardiac progenitor cells alleviates left ventricular dysfunction in rats with a 30-day-old infarction. Circulation. 2010; 121:293–305. [PubMed: 20048209]
9. Dawn B, Stein AB, Urbanek K, Rota M, Whang B, Rastaldo R, Torella D, Tang XL, Rezazadeh A, Kajstura J, Leri A, Hunt G, Varma J, Prabhu SD, Anversa P, Bolli R. Cardiac stem cells delivered intravascularly traverse the vessel barrier, regenerate infarcted myocardium, and improve cardiac function. Proc Natl Acad Sci U S A. 2005; 102:3766–3771. [PubMed: 15734798]
10. Li Q, Guo Y, Ou Q, Chen N, Wu WJ, Yuan F, O'Brien E, Wang T, Luo L, Hunt GN, Zhu X, Bolli R. Intracoronary administration of cardiac stem cells in mice: A new, improved technique for cell therapy in murine models. Basic Res Cardiol. 2011; 106:849–864. [PubMed: 21516491]
11. Tang XL, Li Q, Rokosh DG, Chen N, Sanganalmath SK, Stowers H, Hunt G, Bolli R. The beneficial effects of cardiac stem cell therapy on left ventricular function and structure persists for at least one year in rats with acute myocardial infarction. Circulation. 2012; 126:A12248.
12. Bolli R, Tang XL, Sanganalmath SK, Rimoldi O, Mosna F, Abdel-Latif A, Jneid H, Rota M, Leri A, Kajstura J. Intracoronary delivery of autologous cardiac stem cells improves cardiac function in a porcine model of chronic ischemic cardiomyopathy. Circulation. 2013; 128:122–131. [PubMed: 23757309]
13. Bolli R, Chugh AR, D'Amario D, Loughran JH, Stoddard MF, Ikram S, Beache GM, Wagner SG, Leri A, Hosoda T, Sanada F, Elmore JB, Goichberg P, Cappetta D, Solankhi NK, Fahsah I, Rokosh DG, Slaughter MS, Kajstura J, Anversa P. Cardiac stem cells in patients with ischaemic cardiomyopathy (scipio): Initial results of a randomised phase 1 trial. Lancet. 2011; 378:1847–1857. [PubMed: 22088800]
14. Chugh AR, Beache GM, Loughran JH, Mewton N, Elmore JB, Kajstura J, Pappas P, Tatooles A, Stoddard MF, Lima JA, Slaughter MS, Anversa P, Bolli R. Administration of cardiac stem cells in patients with ischemic cardiomyopathy: The scipio trial: Surgical aspects and interim analysis of myocardial function and viability by magnetic resonance. Circulation. 2012; 126:S54–S64. [PubMed: 22965994]
15. Rota M, Padin-Iruegas ME, Misao Y, De Angelis A, Maestroni S, Ferreira-Martins J, Fiumana E, Rastaldo R, Arcarese ML, Mitchell TS, Boni A, Bolli R, Urbanek K, Hosoda T, Anversa P, Leri A, Kajstura J. Local activation or implantation of cardiac progenitor cells rescues scarred infarcted myocardium improving cardiac function. Circ Res. 2008; 103:107–116. [PubMed: 18556576]
16. D'Amario D, Fiorini C, Campbell PM, Goichberg P, Sanada F, Zheng H, Hosoda T, Rota M, Connell JM, Gallegos RP, Welt FG, Givertz MM, Mitchell RN, Leri A, Kajstura J, Pfeffer MA, Anversa P. Functionally competent cardiac stem cells can be isolated from endomyocardial biopsies of patients with advanced cardiomyopathies. Circ Res. 2011; 108:857–861. [PubMed: 21330601]
17. Stein AB, Tiwari S, Thomas P, Hunt G, Levent C, Stoddard MF, Tang XL, Bolli R, Dawn B. Effects of anesthesia on echocardiographic assessment of left ventricular structure and function in rats. Basic Res Cardiol. 2007; 102:28–41. [PubMed: 17006633]
18. Mohsin S, Khan M, Toko H, Bailey B, Cottage CT, Wallach K, Nag D, Lee A, Siddiqi S, Lan F, Fischer KM, Gude N, Quijada P, Avitabile D, Truffa S, Collins B, Dembitsky W, Wu JC, Sussman MA. Human cardiac progenitor cells engineered with pim-i kinase enhance myocardial repair. J Am Coll Cardiol. 2012; 60:1278–1287. [PubMed: 22841153]
19. Iso Y, Rao KS, Poole CN, Zaman AK, Curril I, Sobel BE, Kajstura J, Anversa P, Spees JL. Priming with ligands secreted by human stromal progenitor cells promotes grafts of cardiac stem/progenitor cells after myocardial infarction. Stem Cells. 2014; 32:674–683. [PubMed: 24022988]
20. Kajstura J, Bai Y, Cappetta D, Kim J, Arranto C, Sanada F, D'Amario D, Matsuda A, Bardelli S, Ferreira-Martins J, Hosoda T, Leri A, Rota M, Loscalzo J, Anversa P. Tracking chromatid

segregation to identify human cardiac stem cells that regenerate extensively the infarcted myocardium. Circ Res. 2012; 111:894–906. [PubMed: 22851539]

21. Padin-Iruegas ME, Misao Y, Davis ME, Segers VF, Esposito G, Tokunou T, Urbanek K, Hosoda T, Rota M, Anversa P, Leri A, Lee RT, Kajstura J. Cardiac progenitor cells and biotinylated insulin-like growth factor-1 nanofibers improve endogenous and exogenous myocardial regeneration after infarction. Circulation. 2009; 120:876–887. [PubMed: 19704095]
22. Molgat AS, Tilokee EL, Rafatian G, Vulesevic B, Ruel M, Milne R, Suuronen EJ, Davis DR. Hyperglycemia inhibits cardiac stem cell-mediated cardiac repair and angiogenic capacity. Circulation. 2014; 130:S70–S76. [PubMed: 25200058]
23. Zhang LX, DeNicola M, Qin X, Du J, Ma J, Tina Zhao Y, Zhuang S, Liu PY, Wei L, Qin G, Tang Y, Zhao TC. Specific inhibition of hdac4 in cardiac progenitor cells enhances myocardial repairs. Am J Physiol Cell Physiol. 2014; 307:C358–C372. [PubMed: 24944198]
24. Strauer BE, Steinhoff G. 10 years of intracoronary and intramyocardial bone marrow stem cell therapy of the heart: From the methodological origin to clinical practice. J Am Coll Cardiol. 2011; 58:1095–1104. [PubMed: 21884944]
25. Dib N, Khawaja H, Varner S, McCarthy M, Campbell A. Cell therapy for cardiovascular disease: A comparison of methods of delivery. J Cardiovasc Transl Res. 2011; 4:177–181. [PubMed: 21181320]
26. Iwasaki H, Kawamoto A, Ishikawa M, Oyamada A, Nakamori S, Nishimura H, Sadamoto K, Horii M, Matsumoto T, Murasawa S, Shibata T, Suehiro S, Asahara T. Dose-dependent contribution of cd34-positive cell transplantation to concurrent vasculogenesis and cardiomyogenesis for functional regenerative recovery after myocardial infarction. Circulation. 2006; 113:1311–1325. [PubMed: 16534028]
27. Shim WS, Tan G, Gu Y, Qian L, Li S, Chung YY, Lim SY, Sim E, Chuah SC, Wong P. Dose-dependent systolic contribution of differentiated stem cells in post-infarct ventricular function. J Heart Lung Transplant. 2010; 29:1415–1426. [PubMed: 20688539]
28. Shen D, Cheng K, Marban E. Dose-dependent functional benefit of human cardiosphere transplantation in mice with acute myocardial infarction. J Cell Mol Med. 2012; 16:2112–2116. [PubMed: 22225626]
29. Wolf D, Reinhard A, Seckinger A, Katus HA, Kuecherer H, Hansen A. Dose-dependent effects of intravenous allogeneic mesenchymal stem cells in the infarcted porcine heart. Stem Cells Dev. 2009; 18:321–329. [PubMed: 18435573]
30. Dawkins J, Gallet R, Kreke M, Smith R, Middleton RJV, Cingolani E, Kar S, Marban L, Makkar R, Marban E. Dose-escalation study using novel continuous flow intracoronary delivery of allogeneic cardiosphere-derviced stem cells: Is there a threshold for cell therapy? Circulation. 2014; 130:A16451. (Abstract).

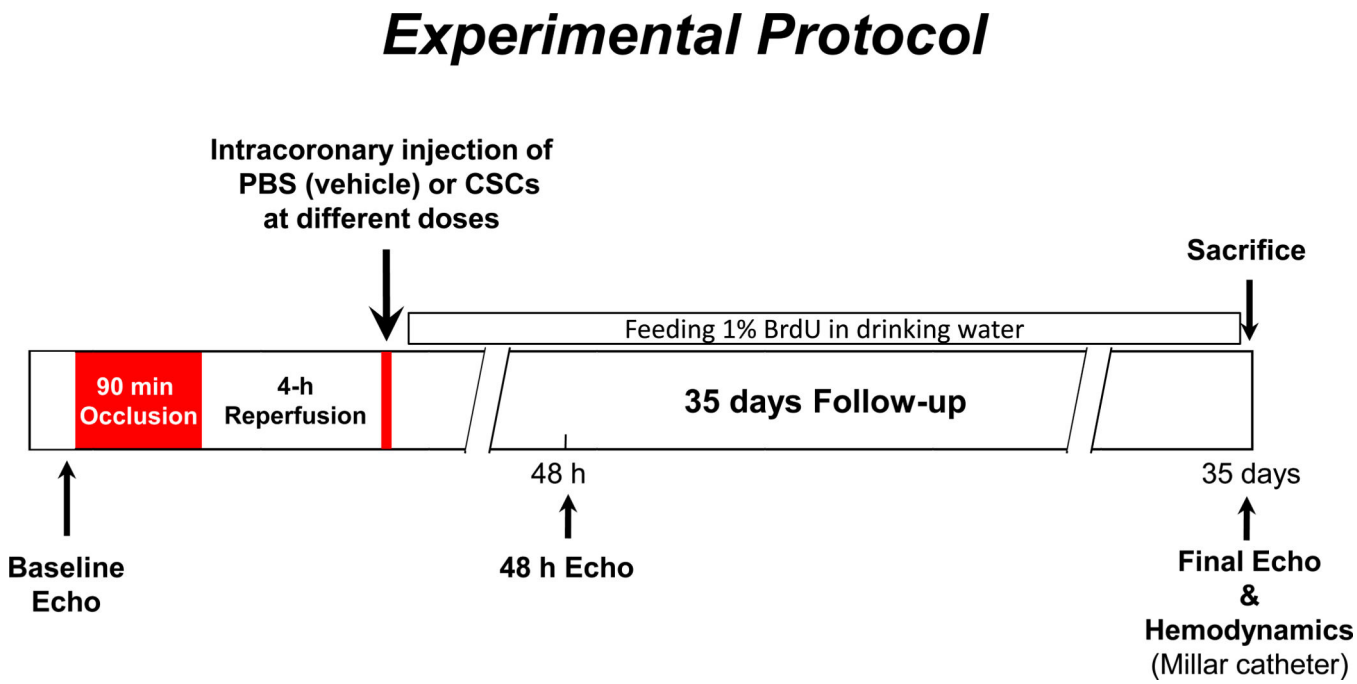

Figure 1. Experimental protocol

Fischer 344 female rats (age 3–4 months)

GFP-labeled syngeneic CSCs were injected into the aortic root during two 20-s occlusions of the ascending aorta and pulmonary artery, 10 min apart , and a 0.5 ml of volume was delivered each injection (CSCs were suspended in a total of 1.0 ml medium for each rat)

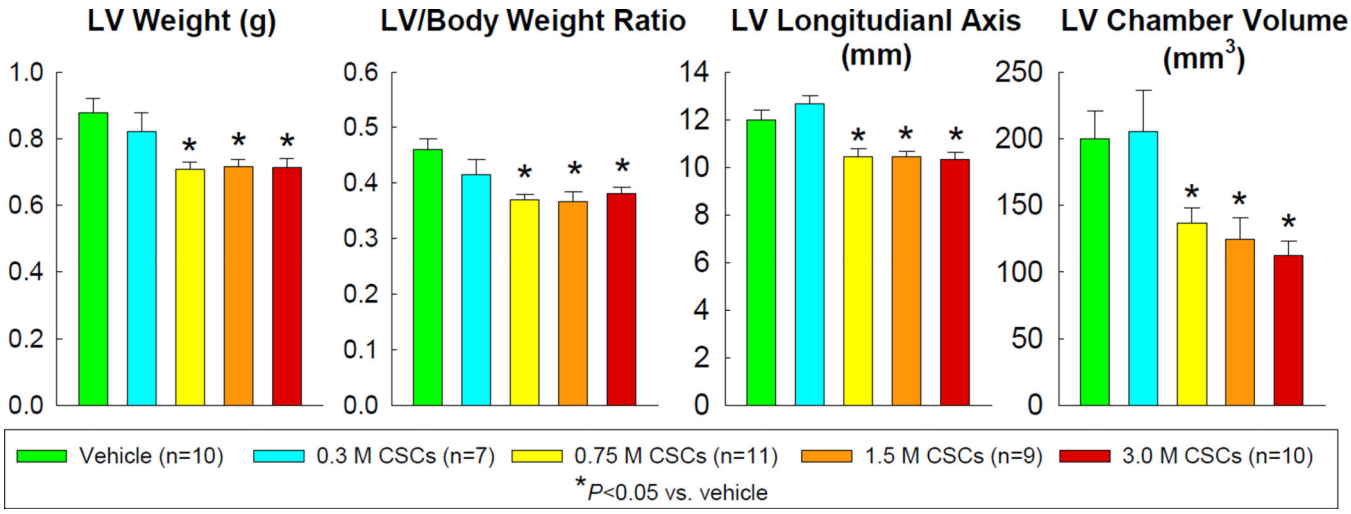

Figure 2.

Postmortem gross measurements were conducted in perfused hearts arrested in diastole. Data are means ± SEM.

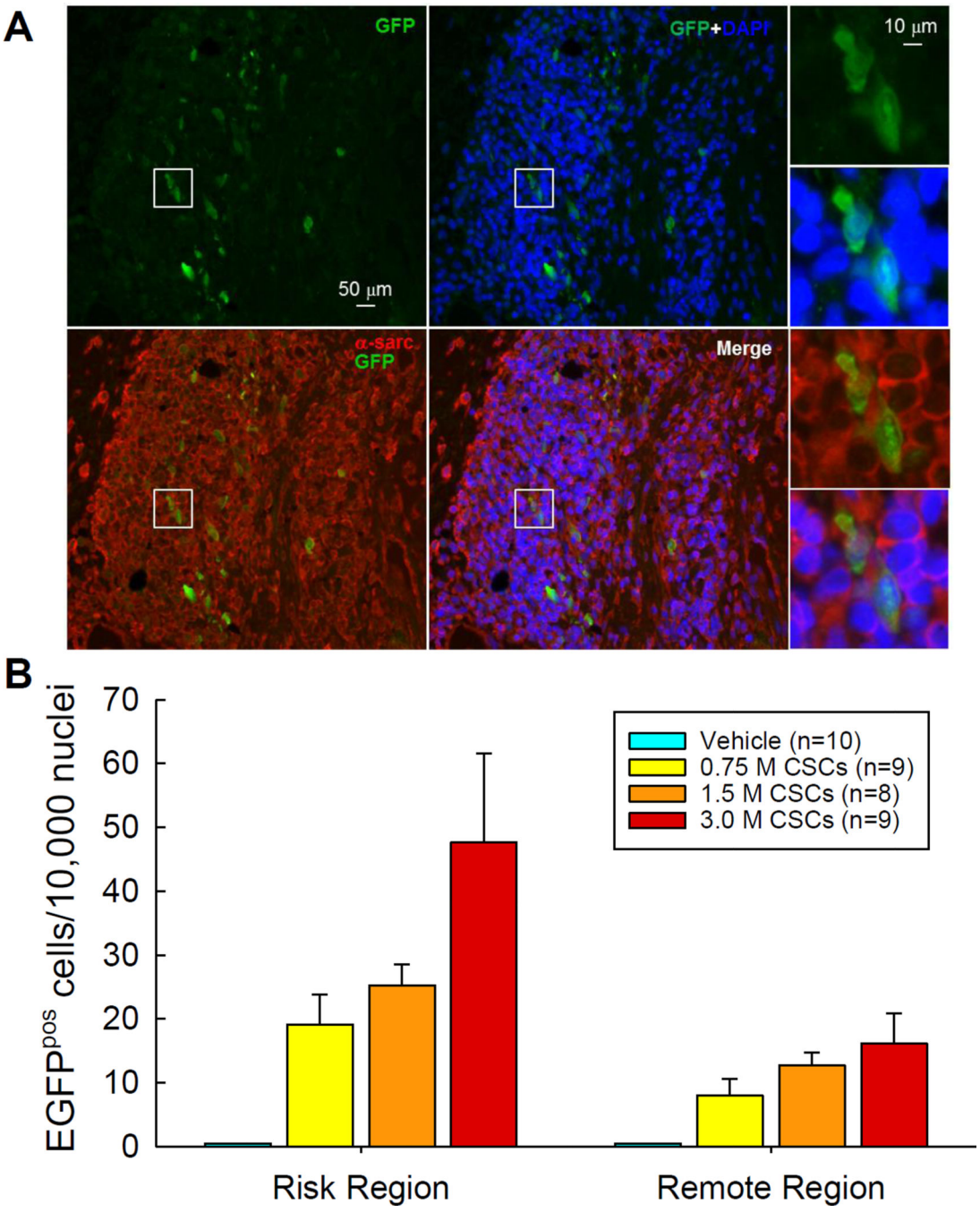

Figure 3. Myocardial engraftment of transplanted CSCs

(***A***). Representative images showing GFP^{pos} cells in the border zone of the LV section from a rat that received 3.0×10^6 CSCs. (***B***). Quantitative analysis was performed in the hearts with detectable GFP^{pos} cells. Data are means ± SEM.

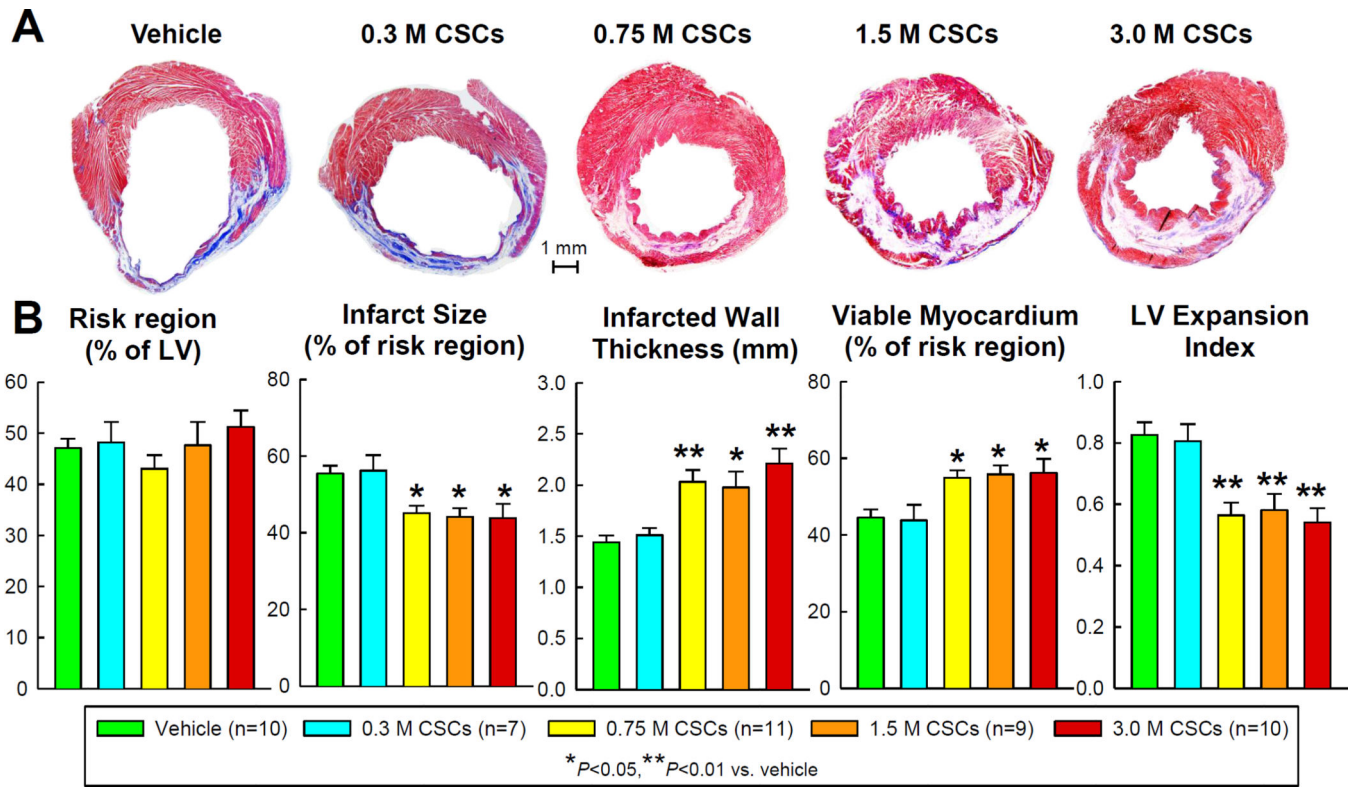

Figure 4. Morphometric analysis

(A). Representative Masson's trichrome-stained LV sections from each of the six groups. Scar tissue and viable myocardium are identified in blue/white and red, respectively. ***(B)***. Quantitative analysis of LV morphometric parameters. The thickness of the infarcted wall was determined by averaging five measurements of LV wall thickness equally distributed within the infarcted LV region; risk region was defined as the LV area between the two edges of the infarct scar; and LV expansion index was calculated as (LV endocardial circumference/LV epicardial circumference) × (non-infarcted region wall thickness/risk region wall thickness). Data are means ± SEM.

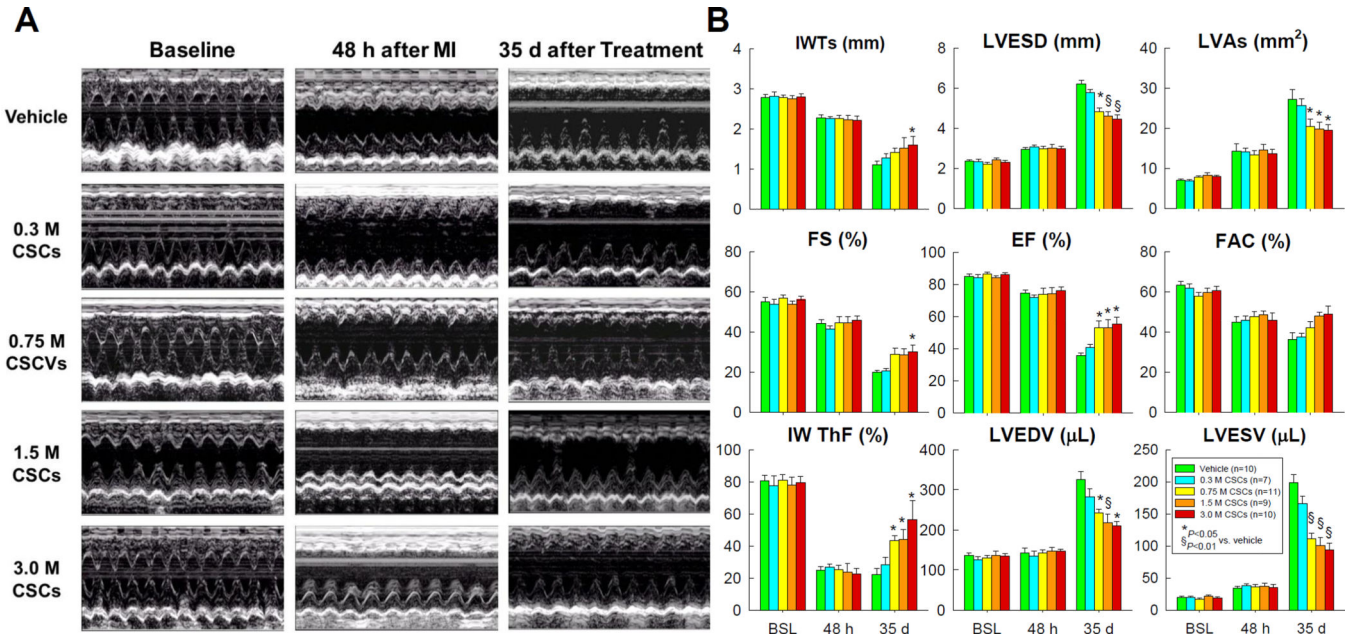

Figure 5. Echocardiographic assessment of LV function

(A) Representative M-mode images from the vehicle, 0.3 $\times 10^6$, 0.75 $\times 10^6$, 1.5 $\times 10^6$, and 3.0 $\times 10^6$, groups recorded at baseline (before MI), 48 h after MI, and 35 d after vehicle or CSC treatment. ***(B)***. Quantitative analyses of echocardiographic parameters at baseline (BSL), 48 h after MI (48 h), and 35 d follow-up (35 d). **IWTs**, systolic infarcted wall thickness; **LVESD**, left ventricular end-systolic diameter; **LVAs**, left ventricular end-systolic area; **FS**, fractional shortening; **EF**, ejection fraction; **FAC**, fractional area change; **IW ThF**, infarcted wall thickening fraction; **LVEDV**, left ventricular end-diastolic volume; and **LVESV**, left ventricular end-systolic volume. Data are means ± SEM.

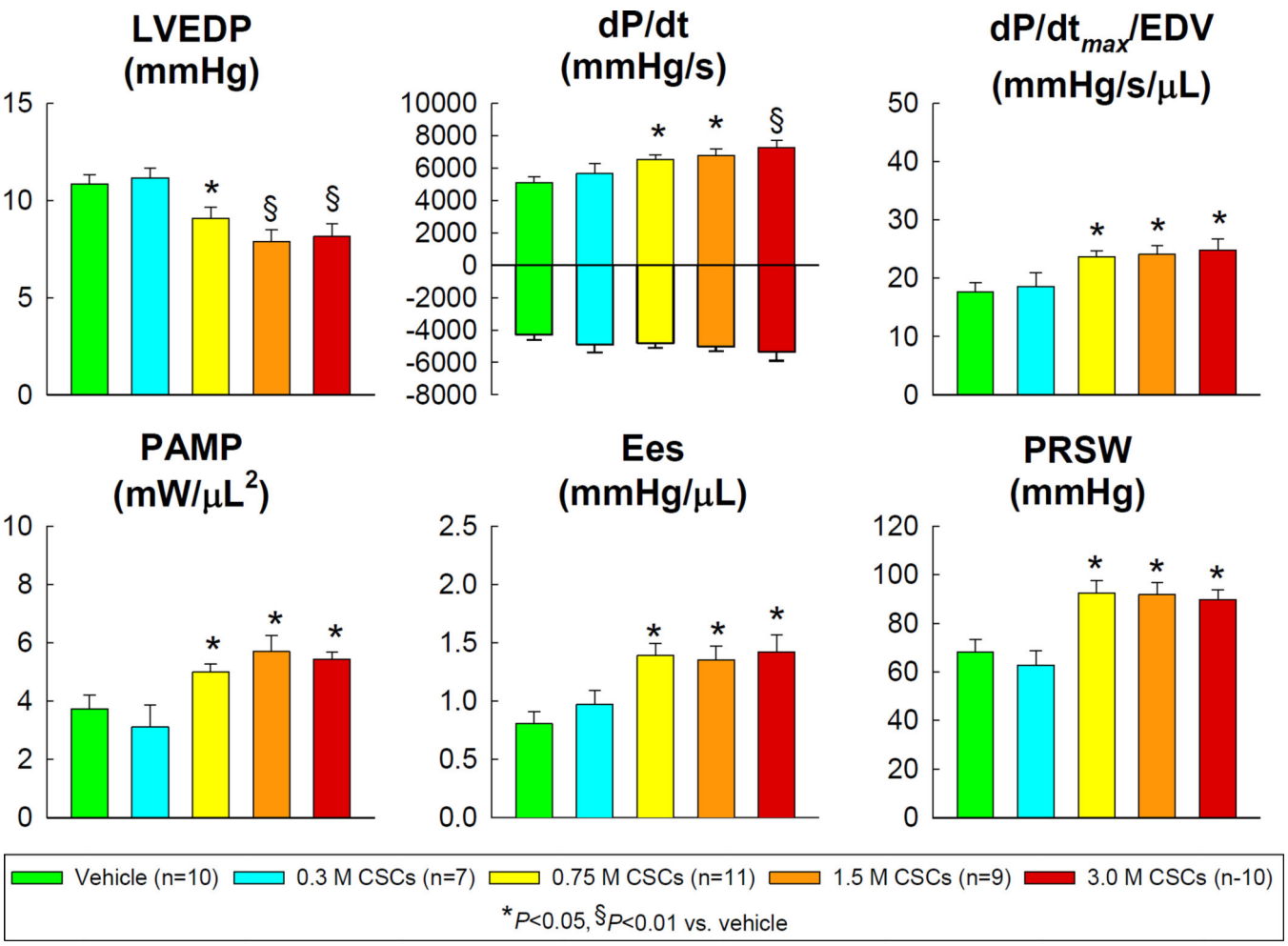

Figure 6.

Hemodynamic assessment of LV function at 35 d follow-up. **LVEDP,** left ventricular end-diastolic pressure; **PAMP,** preload adjusted maximal power; **Ees**, end-systolic elastance; and **PRSW**, preload recruitable stroke work. Data are means ± SEM.

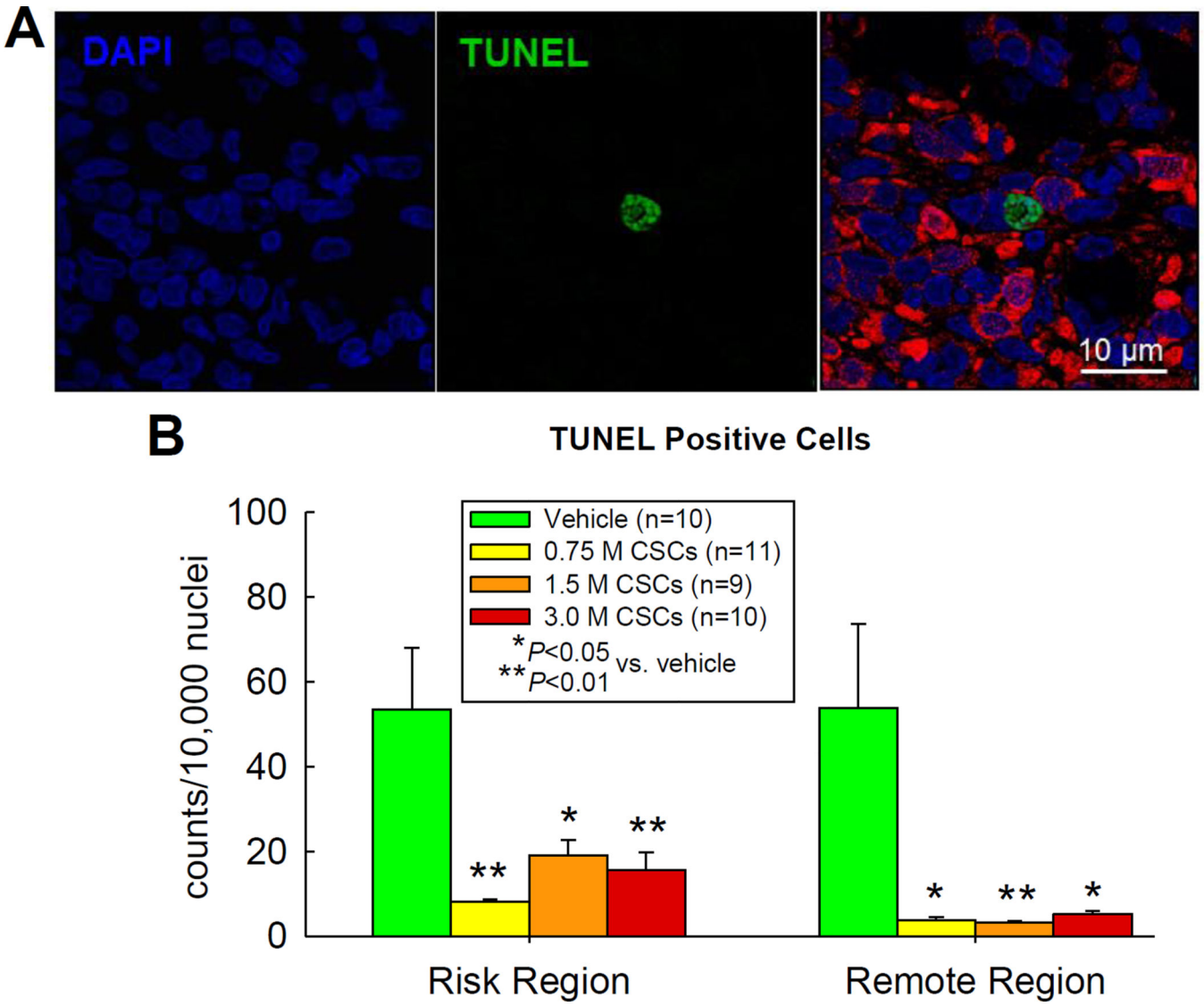

Figure 7. Analysis of apoptosis by TUNEL staining

(A) Representative confocal microscopic images in the border zone of a 3.0 ×10^6 CSC-treated rat showing TUNEL positive nuclei (green), DAPI staining (blue), and a merge of TUNEL and DAPI staining; ***(B)*** Quantitative analysis of TUNEL positive nuclei in the risk and remote (noninfarcted) region in the vehicle- and three doses of CSC-treated groups. Data are means ± SEM.

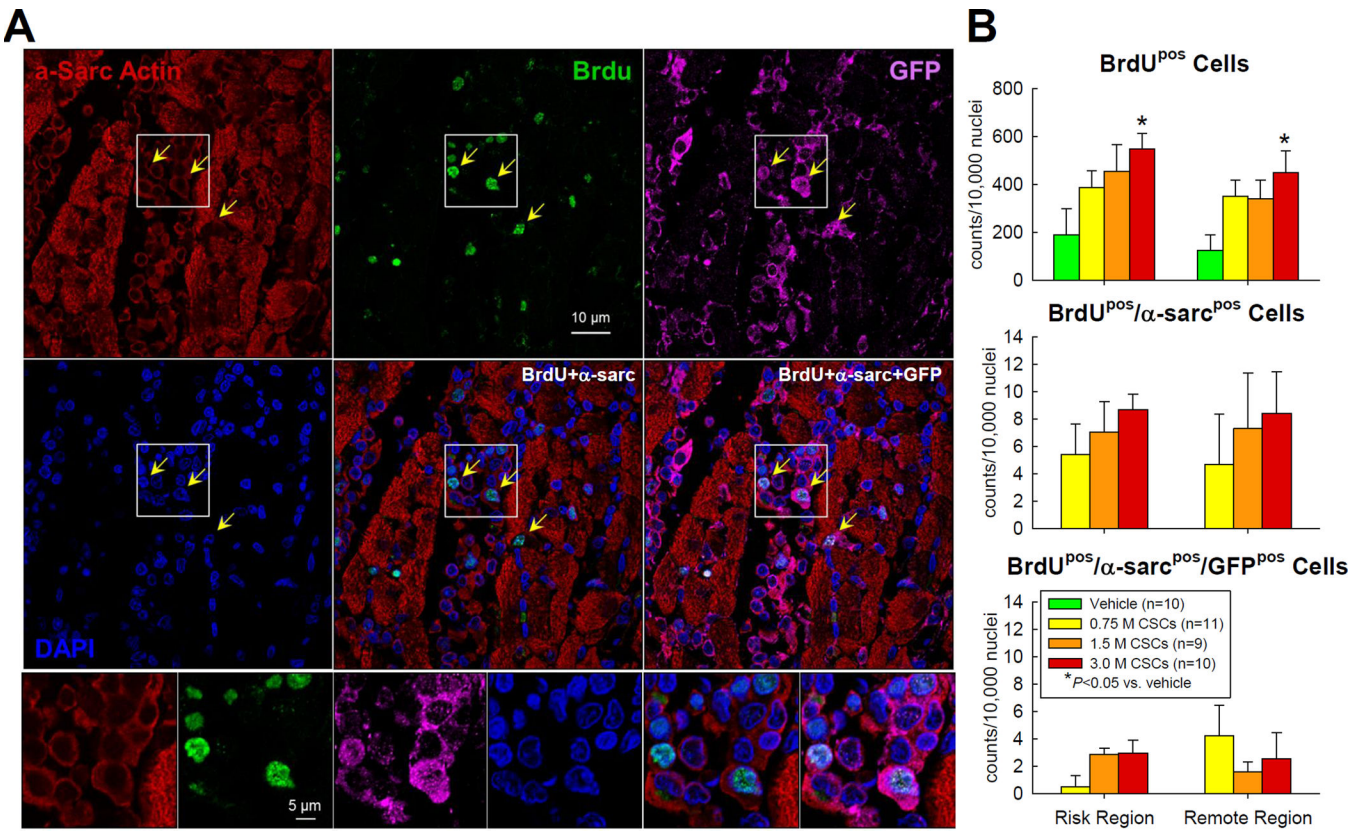

Figure 8. Proliferation of transplanted CSCs

(***A***) Representative confocal microscopic images from a 3.0 ×10^6 CSC-treated rat showing BrdU uptake in the infarcted region during the 35 d follow-up. **Yellow arrows** indicate GFP^{pos} cells that are BrdU positive. ***(B)*** Quantitative analysis of $BrdU^{pos}$ cells, $BrdU^{pos}$/α-$sarc^{pos}$ cells (cells with colocalization of BrdU [FITC] and α-sarcomeric actin [TRITC]), and $BrdU^{pos}$/α-$sarc^{pos}$/GFP^{pos} cells (cells with colocalization of BrdU [FITC], α-sarcomeric actin [TRITC], and GFP [TRITC]) in the risk and remote (noninfarcted) regions. Data are means ± SEM.

Table

Enrollment and Exclusion

Group	Animals Initial Enrollment	Exclusion Due to Death	Animals Completed Protocol	Mortality (%)
Vehicle	14	4	10	28.6*
0.3 ×10^6 CSCs	10	3	7	30.0*
0.75 ×10^6 CSCs	15	4	11	26.7*
1.5 ×10^6 CSCs	13	4	9	30.8*
3.0 ×10^6 CSCs	15	5	10	33.3*
6.0 ×10^6 CSCs	15	12	3	80.0
Total	**82**	**32**	50	**39.0**

* $P<0.05$ vs. 6.0 ×10^6 CSCs